Websites:
http://www.sciencepub.net/newyork
http://www.sciencepub.net

Emails:
newyorksci@gmail.com
editor@sciencepub.net

New York Science Journal

MARSLAND PRESS
Multidisciplinary Academic Journal Publisher

Radioactivity and mineralogy of microgranite dykes and stream sediments of Ras Abda Area, northern Eastern Desert, Egypt.

Fatma S. Ramadan[1], Ali A. Omran[2], Hesham A. El-Nahas[2],Ehab K. Abu Zeid[2], Mohamed Hassan[2,*]

[1] Geology Dept., Fac. Sci., Zagazig Univ., P.O. Box: 44511 Zagazig, Egypt.
[2] Nuclear Materials Authority; P.O. Box: 530 El-Maadi, Cairo, Egypt.
*Correspondence: geo.mohamedhassan86@gmail.com
Authors' Emails: Fatma_r@yahoo.com, A_Omran@yahoo.com, Hesham_nahas@yahoo.com, Ehab_zeid@yahoo.com, geo.mohamedhassan86@gmail.com

Abstract: Ras Abda Area is located in the north part of the Eastern desert, and is characterized by a rugged topography and high relief. The main exposed rock units in the area comprise older granites, younger gabbros and younger granites as well as several types of post granite dykes as rhyolite and bascic dykes in addition to microgranite dykes. Radiometric measurements indicated that the microgranite samples are characterized by anomalous concentrations of the radioelements where eU varies from 29 to 820 ppm, with an average 267 ppm, and eTh ranges between 143 to 5730 ppm with an average 1010.2 ppm. The ratio eTh/eU fluctuates between natural (3.3 & 3.6) and high ratios (4.33 to 10.7) with a general average about 5.6 (higher than the world average of 3.5) indicating that the rocks originated from radio elements-bearing magma and may be subjected to epigenetic processes of leachability and migration of uranium. The selected samples of stream sediments (10 samples) show low levels of radioactivity where eU ranges from 4.0 to 7ppm with an average 5.3ppm, and eTh ranges from 6.0 to 18.0 ppm with an average 10.65ppm. The eTh/eU ratio ranges from 1.2 to 3.6 where the sample distal from the microgranite dykes characterized by the highest ratio (3.6) while those close to the dykes have the lower ratios. Generally, the average eTh/eU ratio (about 2.08) is lower than the world ratio (3.5) indicating that uranium may be enriched from an adjacent source may be the microgranite dykes. The calculated factors of equilibrium (P and D) indicated disequilibrium state for both samples types (microgranite and stream sediments) referring to incomplete U-decay series. Mineralogical studies revealed that the heavy minerals could be classified into: a) radioactive minerals comprising uranophane, kasolite, sklodowskite, thorite and uranothorite, and b) radioelements-bearing minerals comprising columbite, fergusonite, samarskite, pyrochlore, allanite, monazite, zircon and fluorite. The heavy minerals are mostly concentrated upstream rather than downstream; meandering portion of the stream may act as natural traps for the heavy minerals.

[Fatma S. Ramadan, Ali A. Omran, Hesham A. El-Nahas, Ehab K. Abu Zeid, Mohamed Hassan. **Radioactivity and mineralogy of microgranite dykes and stream sediments of Ras Abda Area, northern Eastern Desert, Egypt.** *N Y Sci J* 2019;12(11):35-46]. ISSN 1554-0200 (print); ISSN 2375-723X (online). http://www.sciencepub.net/newyork. 5. doi:10.7537/marsnys121119.05.

Key words: Ras Abda; North Eastern Desert; Egypt; microgranite; radioactivity; mineralogy.

1. Introduction

The high radioactivity level of the basement rocks of Egypt is attributed to the presence of radioactive accessory minerals (Schürmann, 1966). El Hadary et al. (2010), and Abdel Hamid et al. (2018) reported that the mineralized microgranite is highly radioactive due to presence of minerals as zircon, monazite, thorite, uranothorite and allanite.

Ras Abda area is located in the Northern Eastern Desert of Egypt at, about 20 km westward from Safaga City at the Red Sea coast. The area can be easily accessed via a newly established part of Qena–Safaga asphaltic road, which runs directly to the north of the area. The study area is bounded by latitudes 26° 43ˉ 20ˉˉ and 26° 43ˉ 33ˉN and longitudes 33° 45ˉ 31ˉˉ and 33° 45ˉ 49ˉˉ E (Fig. 1). The area is characterized by moderate to high topography relative to its surroundings.

Most of the previous studies on this locality are focused on field relationships, petrographical, mineralogical and geochemical studies besides uranium-thorium distribution investigations applied to samples collected from the less altered and mineralized parts of Wadi Ras Abda microgranite (Omran et al. 2016). There are few detailed investigations on stream sediment. The previous

radiometric investigations were based on air- borne radiometric surveys (Ahmed, 2018).

The geology of Ras Abda area and its surrounding, the structural framework and their potentialities for mineralizations have been discussed by several workers. Omran (2015), stated that Ras Abda area is occupied with Precambrian basement suites comprise older older granitoids and younger gabbro which are injected with basic and acidic dykes of different attitudes. The basic dykes are the oldest and the prevalent ones. They are mainly basaltic in composition. He also recorded for the first time the presence of highly radioactive poly-mineralized granite offshoots in the area, (Fig. 1).

The main purpose of the present study is to outline the surface radiometric anomalies. Wadi deposits and granitic dykes were carefully surveyed and samples studied radiometrically using different techniques.

1. Geological Setting

The area is mostly dominated by the older granitoid rocks ranging in composition from granodiorite to quartz diorite. They are intruded by young gabbro in the northern part. The younger granites are present as small bodies intruding the older granite in the southern part and as a microgranitic off-shoots outcropping in the central part of the area (Fig.1).

The basic dykes are intersected by acidic ones. The acidic dykes are less abundant but the largest in terms of size and space compared to the basic ones. They are mainly of rhyolite, and microgranite composition. They are encountered at the northeastern part and extend to the southwestern part of the area. Also, the rhyolite dykes occupy the middle area and extend from the extreme southwest to the northeast. They form high and huge blocks, with irregular shapes.

At the western part of wadi Ras Abda, the microgranitic dykes are present as swarms of abnormal high radioactivity and poly-mineralization. They are restricted to a highly deformed, faulted, and sheared narrow zone. The zone has been split into two parts under the action of a NW-SE left lateral strike-slip fault (Fig.1).

2. Materials and methods

Geological maps, and satellite images have been used to delineate the radiometric anomalous areas in the present study. Landsat Multispectral Scanner (MSS) and thematic Mapper (TM) images enable the investigation of land systems and geological terrains over large areas. The discrimination potential of multispectral image data depends mainly on the wavelength range and spectral resolution of remote sensing instrument.

Six samples from the microgranite dykes were collected beside ten grab samples from the stream sediments were selected to measure the Uranium (eU), thorium (eTh), radium (Ra) and potassium (K^{40}) contents radiometrically.

Stream sediment samples were prepared for analyses by drying to remove the water content, splitting using the John's splitter and rotary splitter to obtain a representative batch. Rock samples are crushed to about 1mm grain size, a portion of the sample weighting about 300-400 g stored in plastic containers, sealed well and left for 30 days to accumulate free radon to attain radioactive equilibrium (Matolin, 1991).

The measurement of eU, eTh, Ra and K^{40} were carried out in the laboratories of Nuclear Material Authority (NMA), Egypt, using of a Bicron Scintillation Detector NaI (TI), The radioelements concentrations were also measured chemically using the Inductive Coupled Plasma Mass Spectrometer (ICP-MS) of ACME Lab in Vancouver, Canada.

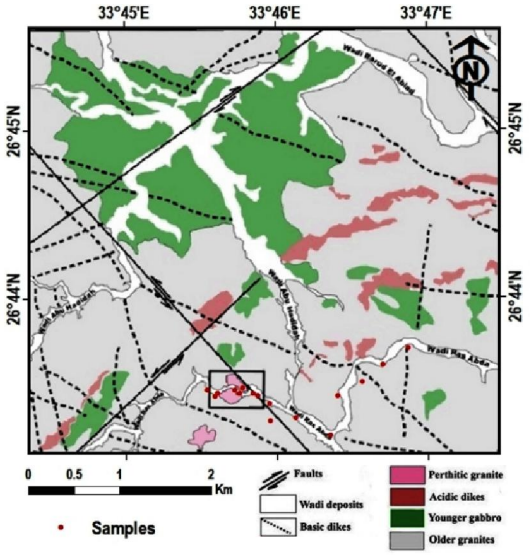

Fig. 1: Geological map of Ras Abda area, Northern Eastern Desert, Egypt (Omran, 2015)

Two conventional heavy liquids were used to concentrate the heavy economic minerals. Bromoform (specific gravity of 2.8 g/cm3) and Methylene Iodide (di-iodomethane) (specific gravity of 3.3 g/cm3). Then the magnetite grains were removed from each concentrate with a hand magnet. Finally the magnetic free heavy parts were subjected to magnetic fractionation using the Frantz Isodynamic Separator (model, L-1). The chosen parameters for magnetic fractionation were side slope of 5°, forward slope of 20°, at different electric current at 0.2, 0.5, 1.0, and 1.5 Ampere. The separated minerals were recognized by stereomicroscope, identified by XRD and confirmed

by electron scanning microscope (ESEM) in the labs of Egyptian Nuclear Materials Authority.

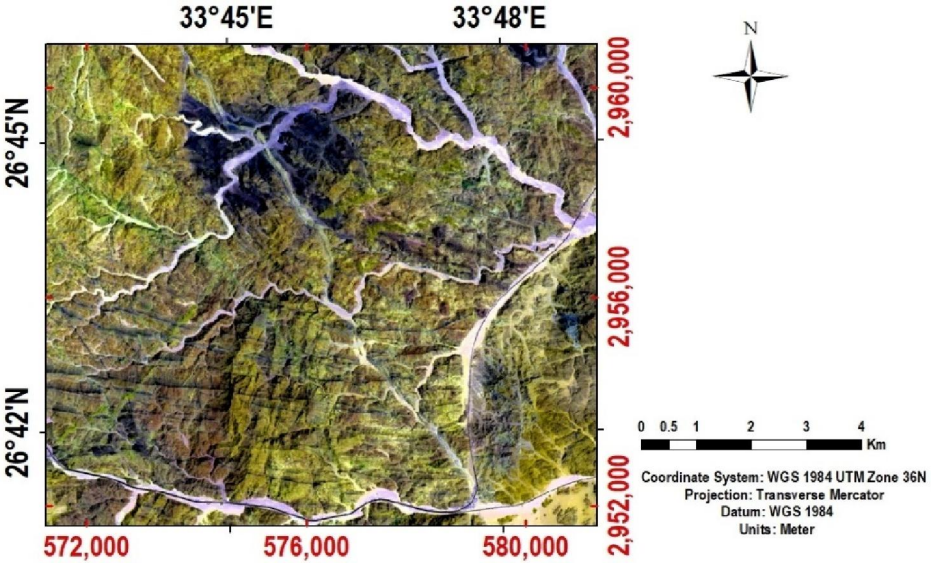

Fig. 2: Landsat composite color image of 7, 6 and 1 bands in RGB colors for Ras Abda area.

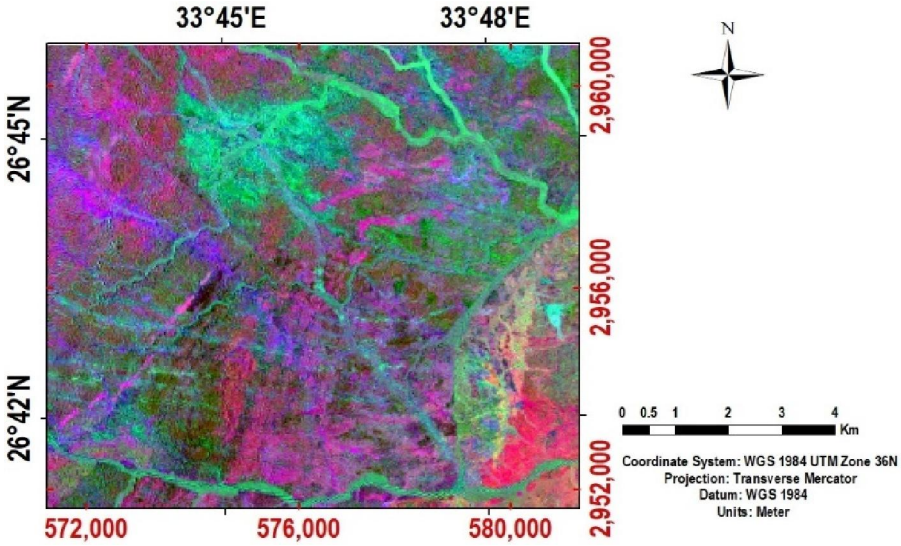

Fig. 3: Lands at false composite color image with band ratios (4/2, 5/6 & 6/7) in RGB colors for Ras Abda area.

3. Results and discussion

3.1. The satellite imagery data

Multispectral remote-sensing has been successfully used for lithological and mineral mapping especially with the development of the remote-sensing sensors and mathematical algorithms that provided detailed information of the mineralogy of the different rock types comprising the earth's surface (Zhang et al., 2007). The detection of hydrothermally altered areas, which are potential sites for mineral deposits using multispectral or hyper-spectral remote sensing was discussed by many authors (Sabins, 1999 and Ferrier, 2002).

For the image analysis of the Landsat-8 (TM) images, a false color composite RGB images were made of bands 7, 6 and 1 and with band ratio 4/2, 5/6 and 6/7, to discriminate the boundary of rock units depending on the color difference and photo geological characteristics of rocks. On the 7, 6, 1 image, the Quaternary deposits of the wadi sediments have a light white color, the older granites are greenish brown, while the younger granites have brown color and the younger gabbro have blue color (Fig. 2). On the band ratio image, reddish areas are rich with iron oxide and represent granites, dark greenish areas are rich with (Fe & Mg) minerals as olivine which

represented gabbro, light greenish areas represent stream sediments and bluish area represent volcanic rocks (Fig. 3).

3.2. Radioactivity

4.2.1 Radiometric measurements

The microgranite samples are characterized by anomalous concentrations of the radioelements: eU varies from 29 to 820 ppm, with an average 267 ppm, and eTh ranges between 143 to 5730 ppm with an average 1010.2 ppm (Table 1). Rogers and Adams (1969) suggested 3.5 to 4 for the Th/U ratios in the world granites. In the present study the ratio eTh/eU fluctuates between natural (3.3 & 3.6) and high ratios (4.33 to 10.7) with general average about 5.6 (higher than the world average of 3.5) indicating that the rock originated from radioelements-bearing magma and may be subjected to epigenetic processes of leachability and migration of uranium. They are considered as the source of radioactive minerals like Zircon, monazite, columbite, fergusenite, thorite and uranothorite.

Table 1: Radiometric measurements of eU, eTh, Ra (ppm) & K% for Ras Abda microgranite.

S. No.	eU	eTh	Ra	K^{40}	eTH/eU	eU/Ra
T1	**175**	**875**	**111**	**5.7**	**5.0**	**1.6**
T2	**483**	**1724**	**183**	**0.6**	**3.6**	**2.6**
T3	**615**	**1999**	**240**	**12.1**	**3.3**	**2.6**
T4	**820**	**5730**	**342**	**0.6**	**7.0**	**2.4**
T5	**33**	**143**	**17**	**2.7**	**4.33**	**1.9**
T6	**29**	**310**	**27**	**0.8**	**10.7**	**1.1**
Average	**267**	**1010.2**	**115.6**	**3.7**	**5.6**	**1.9**

The stream sediment samples show low level of radioactivity where eU ranges from 4.0 to 7 ppm with an average 5.3 ppm, and eTh ranges from 6.0 to 18.0 ppm with an average 10.65 ppm (Table 2). The eTh/eU ratio ranges from 1.2 to 3.6; the sample distal from the microgranite dykes characterized by the highest ratio (3.6) while those close to the dykes have the lower ratios (1.0 to 2.9). Generally, the average eTh/eU ratio (about 2.08) is lower than the world ratio (3.5) indicating that uranium may be enriched from the adjacent source.

Radioactivity is mostly restricted in the inner parts of coarse rock fragments containing detrital radioactive minerals like zircon, monazite, columbite, fergusenite, thorite and uranothorite that may be transported from the adjacent microgranite dykes.

Table 2: Radiometric measurements of eU, eTh & Ra (ppm) and K% for Ras Abda stream sediments.

S. No.	eU	eTh	Ra	K^{40}	eTH/eU	eU/Ra
S1	5	14.5	4	1.3	2.9	1.3
S2	5	18	6	1.9	3.6	0.8
S3	5	11	3	2.0	2.2	1.7
S4	6	15	2	1.5	2.5	3.0
S5	5	6	2	1.2	1.2	2.5
S6	5	7	1	1.5	1.4	5.0
S7	5	10	5	1.2	2.0	1.0
S8	4	8	2	1.7	2.0	2.0
S9	7	7	2	1.4	1.0	3.5
S10	6	12	3	1.7	2.0	2.0
Average	**5.3**	**10.65**	**3.0**	**1.54**	**2.08**	**2.28**

Cathelineau and Holliger (1987) stated that uranium mineralization is affected by different processes (leaching, mobility and redistribution of uranium). These processes are affected by hydrothermal solution and/or supergene fluids, which cause disequilibrium in the radioactive decay series in the U-bearing rocks. The activity ratio (AR) can be used to ascertain the equilibrium state, if the value around the unity (1), there is an equilibrium state. When the value is more or less than the unity, it would indicate a state of disequilibrium (Navas et al., 2002). The radioactive equilibrium of any rock can be determined by the calculation of activity ratio (AR) or equilibrium factor (P_{factor}) which is the ratio of radiometric uranium contents (eU) to the radium content Ra, $\mathbf{P_{factor}}$ = **eU/Ra** (Hussein, 1978; and El-Feky et al., 2011). The ratio calculated for the studied microgranite (Table 1) ranging between 1.1 and 2.6 with an average about 1.9 (>1), indicating disequilibrium in U-decay series.

The stream sediments of Ras Abda are characterized by disequilibrium state with $\mathbf{P_{factor}}$

ranging between 0.8 and 5.0 with an average about 2.28 (>1). Nine samples with $\mathbf{P_{factor}}$ more than the unity and only one approaching the unity indicate that they are recent deposits; and uranium (U^{238} series) may attain the equilibrium state in nearly 1.5M.a. according to Reeves and Brooks (1978).

4.2.2 Geochemistry of U and Th

ICPMS uranium concentrations Uc of the studied microgranites show that Uc (average 363.7ppm) is higher than eU (267ppm) that measured radiometrically (Table3), indicating that U-decay series is incomplete.

A second method for determining the radioactive equilibrium is using the ratio between chemically and radiometric measurements of uranium or $\mathbf{D_{factor}}$, where $\mathbf{D_{factor}}$ **=Uc/eU** [20]. The factor calculated for the microgranite samples ranges between 1.1 and 2.0 with an average 1.5 indicating that the Uc is greater than the eU reflecting a disequilibrium state (Table 3).

Table 3: Chemical analysis of Uc and Uc/eU for Ras Abda microgranite.

Sample No.	Uc	eU	Uc / eU
T1	291.3	175.0	1.7
T2	638.7	483.0	1.3
T3	780.6	615.0	1.3
T4	929.4	820.0	1.1
T5	65.4	33.0	2.0
T6	42.5	29.0	1.5
Average	**363.7**	**267**	**1.5**

The relation between U and Th is helpful to know if there is enrichment or depletion of U and Th. The geochemical behavior of U and Th in the studied microgranitic rocks are examined by plotting a number of variation diagrams. The variation diagrams of resp. eU and eTh with their ratios are used to indicate the amount of U remobilization that occurred within the magmatic plutons (Charbonneau, 1982).

The variation diagram of eU and eTh for the studied microgranitic rocks (Fig.4.a) shows positive correlation which, indicates that magmatic processes played an important role in the concentration of radioelements (Raslan and El-Feky, 2012).

The relation between eU and Uc for the studied microgranites rocks (Fig.4.b) shows strong positive correlation, which indicates that both magmatic processes and hydrothermal solutions played an important role in the concentration of radioelements (Raslan and El-Feky, 2012).

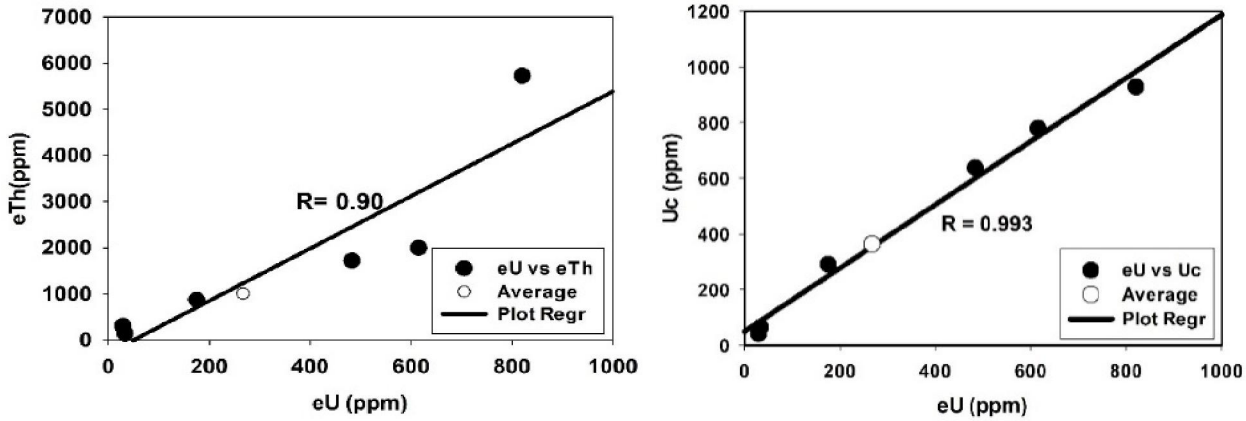

Fig. 4: Variation diagrams of U-Th concentrations for the microgranite of Ras Abda showing: a) eU vs eTh

The variation between eU content and eTh/eU ratios of the microgranites and stream sediments (Figs. 5.a and 5.b) shows negative correlation, which suggests that, the distribution of radioactive elements is not only magmatic but also due to hydrothermal redistribution of radioelements (Raslan and El-Feky, 2012).

4.2.3 Radiometric distribution maps

Using Arc GIS program, four geochemical distribution maps for the concentration of eU, eTh, K^{40} and eRa were constructed and represented in figure (6). From the obtained results of the satellite imagery and the radiometric maps, it is clear that, the highest radioactive zone in the study area is associated with the presence of granitic rocks especially the microgranitic rocks.

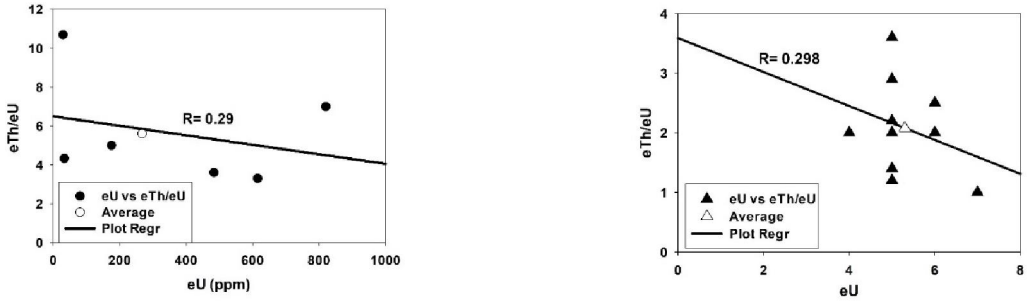

Fig. 5: Variation diagrams of eTh/eU ratio vs eU for the studied rocks of Ras Abda showing: a) eU vs eTh/eU for the microgranite, b) eU vs eTh/eU for the stream sediments

3.3. Mineralogy

The heavy minerals separated from the studied microgranite and stream sediments could be categorized in two groups: **A)** Radioactive minerals and **B)** Radioelements-bearing minerals**.**

4.3.1. Radioactive minerals

This group comprises uranium and thorium bearing minerals and is represented mainly by uranophane, kasolite, sklodowskite, thorite and uranothorite.

1- Uranophane

Uranophane is found in the microgranite samples. The separated grains occur as massive with granular forms ranging in color from yellow to pale canary yellow with dull and greasy luster. The EDX/BSE images are shown in figure (7a), the EDX chemical analysis data is shown in table (4). The X-ray diffraction analysis data is shown in table (5).

Table 4: Chemical analysis of studied (a) Uranophane, (b) Kasolite, (c) Sklodowskite, (d) Thorite, (e) Uranothorite, (f) Columbite, (g) Fergusonite, (h) Samarskite, (i) Pyrochlore, (j) Allanite, (k) Monazite, (l) Zircon and (m) Fluorite minerals from Ras Abda studied samples.

(a) Uranophane		(b) Kasolite		(c) Sklodowskite		(d) Thorite		(e) Uranothorite		(f) Columbite	
Element	Wt %	Element	Wt %	Element	Wt %	Element	Wt %	Element	Wt %	Element	Wt %
Al	2.92			Mg	6.46	Al	1.42	Al	0.83	Al	1.09
Si	11.06			Al	2.53	Si	10.53	Si	6.27	Si	3.06
Ca	7.53	Si	15.89	Si	13.13	Pb	2.03	Ca	3.65	Y	2.43
Ti	6.64	Pb	54.87	P	3.29	U	13.31	Nd	0.82	Ti	3.01
Fe	1.57	U	29.24	K	1.61	Ca	0.69	Ce	1.8	Mn	12.51
Pb	7.88			Ca	0.42	Fe	2.03	Fe	2.85	Fe	4.44
U	62.41			Fe	1.71	Th	64.16	Th	67.04	Ta	2.84
				U	70.86	Zr	5.83	U	11.66	Nb	70.61
								Zr	5.08		
Total	100	Total	100	Total	100	Total	100	Total	100	Total	100
(g) Fergusonite		(h) Samarskite		(i) pyrochlore		(j) Allanite		(k) Monazite		(l) Zircon	
Element	Wt %	Element	Wt %	Element	Wt %	Element	Wt %	Element	Wt %	Element	Wt %
Al	3.13			Al	3.96			Al	0.55	Al	1.9
Si	3.44	Si	3.76	Si	3.87			Si	5.07	Si	23.32
Th	6.55	Y	1.59	U	5.86	Si	19.49	P	18.17	Fe	4.68
U	5.6	Th	3.75	Ca	1.62	Ca	3.46	U	2.25	Hf	2.22
Ca	1.92	Ca	9.34	Ti	0.56	Ti	14.45	Ca	2.59	Zr	67.87
Ti	0.8	Ti	12.35	Ce	1.68	La	14.41	La	15.09	Total	100
Nd	0.39	Nd	1.88	Nd	2.68	Ce	22.42	Pr	3.43	(m) Fluorite	
Dy	5.76	Mn	1.99	Fe	1.95	Pr	1.53	Nd	10.59	Element	Wt %
Er	5.5	Fe	2.31	Co	2.76	Nd	8.64	Ce	28.67		
Yb	6.94	Ta	3.85	Yb	12.58	Sm	1.11	Sm	1.87	F	29.45
Ta	1.84	U	23.48	Ta	3.05	Gd	0.93	Gd	1.21	Si	0.81
Y	17.39	Nb	35.7	Th	5.63	Fe	13.55	Fe	1.2	Y	2.07
Nb	41.51			Y	18.54			Th	9.3	Ca	67.67
				Nb	35.25						
Total	100	Total	100	Total	100	Total	100	Total	100	Total	100

2- Kasolite

This mineral occurs as small prismatic aggregates ranging in color from yellow to yellowish orange with resinous luster recorded in the microgranite samples, The EDX/BSE images are shown in figure (7b), the EDX chemical analysis data is shown in table (4). The X-ray diffraction analysis data is shown in table (5).

3- Sklodowskite

Sklodowskite is recorded in the microgranite samples. The separated grains occur as massive with granular form ranging in color from pale yellow to brownish yellow with dull and earthy luster. The EDX/BSE images are shown in figure (7c), the EDX chemical analysis data is shown in table (4). The X-ray diffraction analysis data is shown in table (5).

4-Thorite

Thorite recorded in stream sediment samples and microgranite rock samples, it has black to brown color and euhedral to subhedral crystals. The EDX/BSE images are shown in figure (7d), the EDX chemical analysis data is shown in table (4). The X-ray diffraction analysis data is shown in table (5).

5- Uranothorite

Uranothorite in the studied area occurs as subhedral to anhedral grains. The majority of uranothorite grains are angular to subrounded prismatic. It recorded in microgranite samples and stream sediment samples beside the microgranite rocks samples. The EDX/BSE images are shown in figure (7e), the EDX chemical analysis data is shown in table (4). The X-ray diffraction analysis data is shown in table (5).

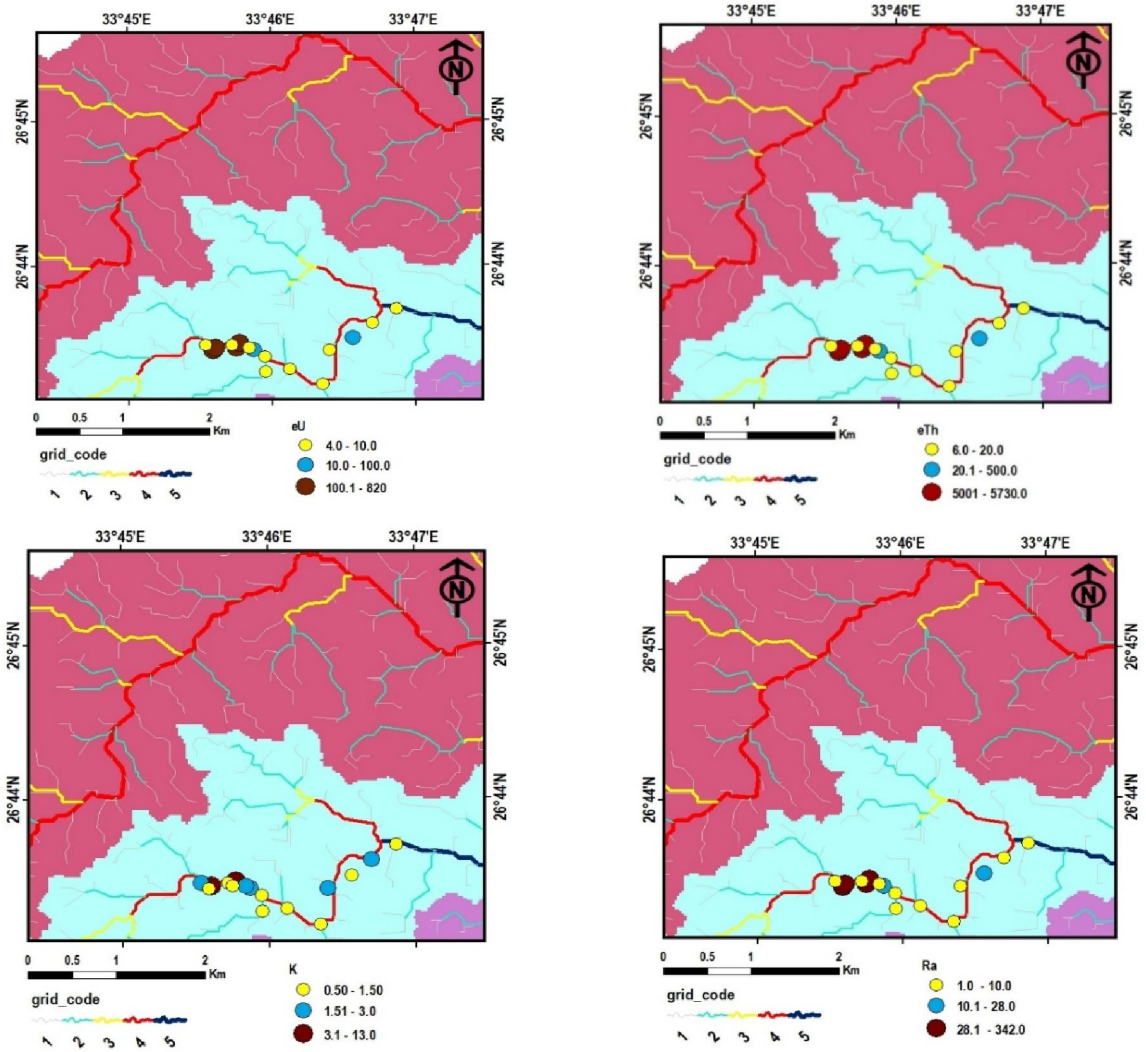

Fig. 6: Geochemical maps showing distribution of the radio elements in the rock units of Ras Abda erea. a) eU (ppm), b) eTh (ppm), c) ^{40}K (ppm) and d) Ra (ppm)

Table 5: X-ray diffraction data of (a) Uranophane, (b) Kasolite, (c) Sklodowskite, (d) Thorite and (e) Uranothorite minerlas from Ras Abda studied samples.

(a) Uranophane				(b) Kasolite				(c) Sklodowskite			
Analyze sample		ASTM card (08-442)		Analyze sample		ASTM card (08-0297)		Analyze sample		ASTM card (29-0875)	
d A°	I/Io	d A°	I/Io	d A°	I/Io	d A°	I/Io	d A°	I/Io	d A°	I/Io
7.90	95	7.88	100	6.50	20	6.61	60	8.49	100	8.42	100
6.61	25	6.61	40	6.11	9	6.19	20	6.43	13	6.37	20
5.40	35	5.42	40	5.25	6	5.31	40	5.93	18	5.91	50
4.82	30	4.76	50	4.20	21	4.19	80	4.84	6	4.82	40
4.27	16	4.29	20	3.53	34	3.53	70	4.35	12	4.33	40
3.93	75	3.94	90	3.35	14	3.38	10	4.20	34	4.19	80
3.59	19	3.60	40	3.25	100	3.26	100	4.06	15	4.00	50
3.51	25	3.51	40	3.06	32	3.07	50	3.54	41	3.52	50
3.21	35	3.20	50	2.92	40	2.93	90	3.26	31	3.27	70
3.00	74	2.99	80	2.73	13	2.73	30	3.00	16	3.00	60
2.91	60	2.91	80	2.64	4	2.64	30	2.89	17	2.87	50
2.70	19	2.69	40	2.36	6	2.73	20	2.79	10	2.80	20
2.63	14	2.63	50	2.18	14	2.18	30	2.12	13	2.13	30
2.20	9	2.20	40	1.96	12	1.69	50	2.09	6	2.09	30
2.10	11	2.10	50	1.74	10	1.74	40	1.97	5	1.98	20
1.97	25	1.96	70	1.86	3	1.68	50				

(d) Thorite				(e) Uranothorite			
Analyze sample		ASTM card (11-419)		Analyze sample		ASTM card (08-393)	
dA°	I/I_o	dA°	I/Io	dA°	I/I_o	dA°	I/Io
4.68	62	4.72	85	4.73	2	4.73	80
3.54	100	3.55	100	3.61	4	3.56	100
2.82	34	2.84	45	1.83	39	1.83	100
2.65	55	2.67	75	1.49	7	1.48	50
2.52	26	2.52	30	1.46	2	1.44	50
2.36	8	2.36	5				
2.20	27	2.22	30				
1.82	33	1.83	65				
1.74	18	1.75	15				
1.65	14	1.66	10				
1.48	8	1.48	20				
1.43	7	1.44	15				

4.3.2. Radioelements-bearing minerals

This group comprises the minerals that are composed mainly of trace elements including the radioelements as substantial constituents. They are represented by the minerals of Nb-Ta series (coluumbite, fergusonite and samarskite) in addition to pyrochlore, allanite, zircon, fluorite and monazite.

1-Coluumbite

The mineral recorded in both stream sediment samples and microgranite rock samples as small black, flattened, short prismatic crystal habit with smooth surface. The mineral have semi-resinous luster. The EDX/BSE images are shown in figure (7f), the EDX chemical analysis data is shown in table (4). The X-ray diffraction analysis data is shown in table (6).

2- Fergusonite

Fergusonite have brown color with no specific crystal shape but usually metamictized**.** The origin of the mineral is considered as the pegmatites and microgranite and it recorded in stream sediment samples and microgranite rock samples. The EDX/BSE images are shown in figure (7g), the EDX chemical analysis data is shown in table (4). The X-ray diffraction analysis data is shown in table (6).

3- Samarskite

Samarskite are generally massive with a granular form. They are characterized by a splendid vitreous or resinous luster. They are mainly of velvet - reddish brown to bloody red in color. They are generally translucent, compact, metamict and hard. Samarskite is usually found in stream sediment samples and microgranite rock samples in appreciable amounts and

distributed in all size fractions with a tendency to increase with decreasing grain size. The EDX/BSE images are shown in figure (7h), the EDX chemical analysis data is shown in table (4). The X-ray diffraction analysis data is shown in table (6).

Table 6: X-ray diffraction data of (a) Columbite, (b) Fergusonite, (c) Samarskite, (d) Pyrochlore, (e) Allanite, (f) Monazite, (g) Zircon and (h) Fluorite minerals from Ras Abda studied samples.

(a) Mangano-Columbite				(b) Fergusonite				(c) Samarskite				(d) Pyrochlore			
Analyze sample		ASTM card (45-1360)		Analyze sample		ASTM card (09-0443)		Analyze sample		ASTM card (10-398)		Analyze sample		ASTM card (13-0254)	
d A°	I/Io	d A°	I/Io	dA°	I/I_o	dA°	I/Io	dA°	I/I_o	dA°	I/Io	d A°	I/Io	d A°	I/Io
7.14	5	7.13	2	3.14	100	3.12	100	4.04	8	4.03	20	3.12	23	3.13	20
3.66	44	3.65	79	3.00	35	3.01	20	3.23	20	3.23	30	2.98	100	3.00	100
2.97	100	2.97	100	2.97	28	2.96	90	3.15	15	3.13	40	2.52	27	2.60	20
2.86	6	2.86	25	2.70	39	2.74	40	2.98	100	2.98	100	2.07	13	2.00	16
2.49	14	2.49	24	2.52	29	2.53	10	2.93	20	2.92	90	1.82	15	1.83	60
2.38	6	2.37	5	2.15	5	2.16	6	2.58	22	2.59	6	1.63	7	1.64	1
2.24	7	2.24	2	1.92	46	1.90	50	2.52	13	2.52	20	1.57	5	1.58	5
2.21	8	2.21	8	1.84	15	1.86	30	1.92	9	1.91	20				
1.77	8	1.77	9	1.64	39	1.65	10	1.87	7	1.86	20				
1.73	13	1.737	16	1.49	8	1.50	6	1.83	39	1.83	20				
1.72	12	7.72	17					1.71	5	1.71	20				
								1.56	30	1.56	30				

(e) Allanite				(f) Monazite				(g) Zircon				(h) Fluorite			
Analyze sample		ASTM card (21-146)		Analyze sample		ASTM card (11-0556)		Analyze sample		ASTM card (06-0266)		Analyze sample		ASTM card (04-0864)	
dA°	I/I°	dA°	I/I°	dA°	I/I_o	dA°	I/I_o	dA°	I/I_o	dA°	I/I_o	dA°	I/I_o	dA°	I/I_o
9.32	20	9.2	40	4.18	13	4.17	25	4.47	25	4.43	45	3.16	100	3.15	94
8.12	12	8.0	40	3.50	22	3.51	25	3.32	100	3.30	100	1.93	40	1.93	100
3.54	46	3.53	50	3.30	83	3.30	50	2.66	3	2.65	8	1.65	6	1.65	35
3.30	6	3.32	20	3.09	100	3.09	100	2.53	35	2.52	45	1.37	3	1.37	12
2.93	100	2.92	100	2.87	25	2.87	70	2.34	10	2.34	10				
2.89	30	2.83	10	2.19	10	2.19	18	2.22	2	2.22	8				
2.72	52	2.71	60	2.15	18	2.15	25	2.07	24	2.07	20				
2.63	41	2.63	50	2.10	7	2.13	25	1.91	9	1.91	14				
2.56	9	2.56	20	1.97	29	1.961	25	1.76	14	1.75	12				
2.14	17	2.14	20					1.72	34	1.71	40				
1.90	8	1.893	20					1.65	19	1.65	14				
1.64	12	1.639	50					1.48	5	1.48	8				
								1.38	11	1.38	10				

4- Pyrochlore

The pyrochlores have a general formula $A_2B_2O_6(O,OH,F)$, where U^{4+} (or U^{6+}) occurs in the A site and B = Ta, Nb (Heinrich, 1958 and Hogarth, 1977). Pyrochlore is present in the microgranite rock samples. The separated grains shown massive metamict brownish red color with adamantine luster. The EDX/BSE images are shown in figure (7i), the EDX chemical analysis data is shown in table (4). The X-ray diffraction analysis data is shown in table (6).

5- Allanite

Allanite recorded in the microgranite rock sample and present in rare percentage in stream sediment samples. It shows a translucent brownish black color, euhedral to subhedral crystals with vitrous luster. The EDX/BSE images are shown in figure (7j), the EDX chemical analysis data is shown in table (4). The X-ray diffraction analysis data is shown in table (6).

6- Monazite

It is a rare earth phosphate of highly variable composition. It exhibits high content from thorium and uranium, therefore, it documented as radioactive mineral. Monazite exhibits shape varies from rounded to oval. Their color ranges from honey to yellowish brown to blue (Fig. 7k). They occur as accessory mineral in the fine sand size fractions in the stream sediments and microgranite. The EDX/BSE images are shown in figure (7k), the EDX chemical analysis

data is shown in table (4). The X-ray diffraction analysis data is shown in table (6).

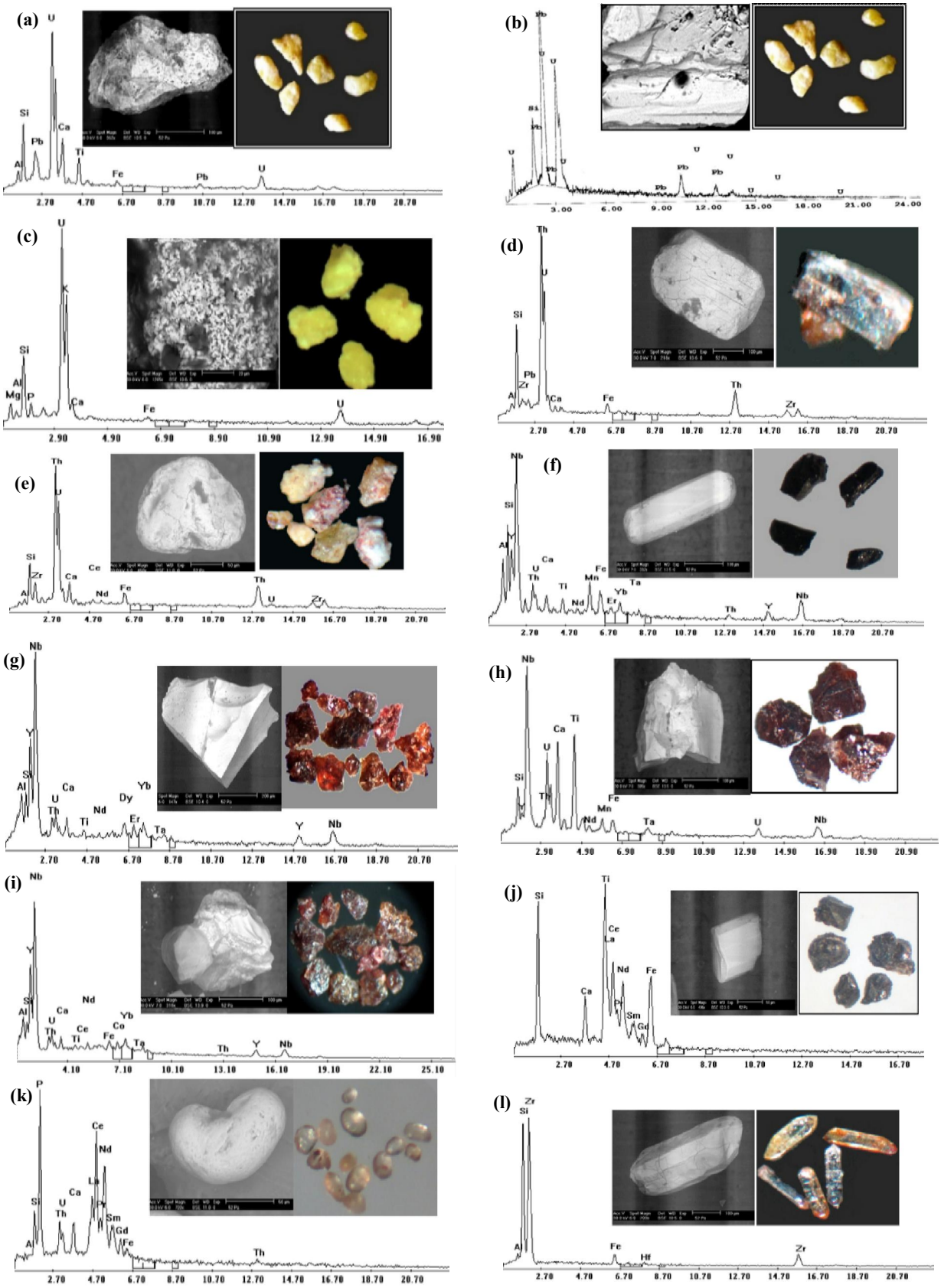

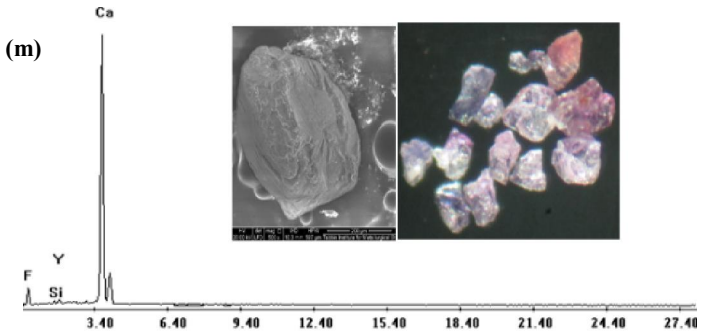

Fig. 7: ESEM spectrograph, BSE image and stereophotograph for (a) Uranophane, (b) Kasolite, (c) Sklodowskite, (d) Thorite, (e) Uranothorite, (f) Columbite, (g) Fergusonite, (h) Samarskite, (i) Pyrochlore, (j) Allanite, (k) Monazite, (l) Zircon and (m) Fluorite minerals from Ras Abda studied samples.

7- Zircon

The separated grains varies in its appearance and color from colorless, pale yellow, reddish yellow and honey with vitreous luster (Fig. 7L). The variation in the color of zircon may be attributed to the density of fine inclusions as well as the degree of iron oxides staining. The EDX/BSE images are shown in figure (7L), the EDX chemical analysis data is shown in table (4). The X-ray diffraction analysis data is shown in table (6).

8- Fluorite

The separated grains occur as massive form ranging in color from colorless to deep violet with vitreous luster. Khazback and Raslan (1995) remarked a positive relation between color of fluorite and the accompanying uranium minerals or to the presence of Y in particular. The EDX/BSE images are shown in figure (7m), the EDX chemical analysis data is shown in table (4). The X-ray diffraction analysis data is shown in table (6).

4. Conclusion

The study concerns microgranite dykes and their effect on the stream sediments of Ras Abda area. The results obtained from the satellite imagery and the radiometric maps show that, the highest radioactive zone in the study area is associated with the presence of granitic rocks especially the microgranite rocks.

Radiometric measurements on samples confirmed this and indicated that the microgranite dykes are characterized by a high radioactivity (average U 267 ppm and average Th 1010.2 ppm). Mineralogically its high radioactivity can be attributed to presence of uranophane, kasolite, sklodowskite, thorite and uranothorite minerals in addition to columbite, fergusonite, samarskite, pyrochlore, allanite, monazite, zircon and fluorite.

The stream sediments are characterized by a low radioactivity (average eU 5.3 ppm and average eTh 10.65 ppm). Their radioactivity is attributed mainly to the radioelements-bearing minerals. Diagentic processes such as mobility leachability and migration of uranium played an essential role in lowering the radioactivity of these sediments. The low radioactivity of the stream sediments is attributed to development of the sediments under condition where uranium contents was removed because of continuous leaching of rock detritus.

Radiometric and geochemical parameters such as eTh/eU ratio indicated the role of epigenetic processes in lowering U-concentration in the microgranite. The ratio eTh/eU of microgranites fluctuates between natural (3.3 & 3.6) and high ratios (4.33 to 10.7) with general average about 5.6 (higher than the world 3.5), indicating that the rock originated from radioelements-rich magma and may be subjected to epigenetic processes of leachability and migration of uranium. The factors P_{factor} and D_{factor} indicated that both the microgranite and stream sediments are in disequilibrium state with incomplete U-decay series.

Authors:

Fatma S. Ramadan, Ali A. Omran, Hesham A. El-Nahas, Ehab K. Abu Zeid, Mohamed Hassan

Affiliation (s) and address (es) of the author (s):

1. **Fatma Sayed Ramadan**
   Professor of geology, Zagazig University, Zagazig, Egypt.
   E-mail: Fatma_r@yahoo.com
   P.O. Box: 44511 Zagazig, Egypt.
2. **Ali Ahmed Omran**
   Professor of geology, Nuclear Materials Authority, Cairo, Egypt.
   E-mail: A_Omran@yahoo.com
   P.O. Box: 530 El-Maadi, Cairo, Egypt.
3. **Hesham Abd El-Aziz El-Nahas**
   Professor of geology, Nuclear Materials Authority, Cairo, Egypt.
   E-mail: Hesham_nahas@yahoo.com
   P.O. Box: 530 El-Maadi, Cairo, Egypt.
4. **Ehab Korany Abu Zeid**

Assistant Professor of geochemistry, Nuclear Materials Authority, Cairo, Egypt.
E-mail: Ehab_zeid@yahoo.com
P.O. Box: 530 El-Maadi, Cairo, Egypt.

5. **Mohamed Hassan (corresponding author)**
Assistant Lecturer, Nuclear Materials Authority, Cairo, Egypt.
E-mail: geo.mohamedhassan86@gmail.com
P.O. Box: 530 El-Maadi, Cairo, Egypt.
Name of corresponding author: **Mohamed Hassan**
Assistant Lecturer, Nuclear Materials Authority, Cairo, Egypt.
E-mail: geo.mohamedhassan86@gmail.com
P.O. Box: 530 El-Maadi, Cairo, Egypt.
Phone number: +2-01120133300

References

1. Schürmann HME. The Precambrian of the Gulf of Suez and the northern part of the Red Sea. E.J. Brill, Leiden. Netherland 1966; 404.
2. EL Hadary A, El Azab A, Omran AA. Contributions to the geology and mineralogy of wadi Ras Abda area, Central Eastern Desert, Egypt. Arab. J. of Sci. 2010; 7: 245-259.
3. Abdel Hamid AA, El Sundoly HI, Abu Steet AA. Hydrothermal alteration and evolution of Zr-Th-U-REE mineralization in the microgranite of Wadi Ras Abda, North Eastern Desert, Egypt. Arab. J. of GeoSci. 2018; 11(11):1-15.
5. Omran AA, Dessouky OK. Ra's Abdah of the north Eastern Desert of Egypt: the role of granitic dykes in the formation of radioactive mineralization, evidenced by zircon morphology and chemistry. Acta Geochimica 2016; 35(4): 368–380.
6. Ahmed SB. Integration of airborne geophysical and satellite imagery data to delineate the radioactive zones at west Safaga Area, Eastern Desert, Egypt. NRIAG J. of Astr. and Geoph. 2018; 7(2): 1-12.
7. Omran AA. Geology, mineralogy and radioelements potentiality of microgranite dikes to the south of wadi abu hadieda area, northern eastern desert Egypt. Al-Azhar Bull Sci. 2015; 26: 67–89.
8. Matolin M. Construction and Use of Spectrometric Calibration Pads Laboratory γ-ray Spectrometry, NMA, Egypt. A Report to the Gov. of ARE. Project EGY1991; 4/030-03, IAEA.
9. Zhang X, Pazner M, Duke N. Lithologic and mineral information extraction for gold exploration using ASTER data in the south Chocolate Mountains (California). Photogram. Rem. Sens. 2007; 62: 271 – 282.
10. Sabins FF. Remote sensing for mineral exploration. Ore. Geol. Rev. 1999; 14: 157-183.
11. Ferrier S. Mapping Spatial Pattern in Biodiversity for Regional Conservation Planning: Where to from Here? Syst. Biol. 2002; 51(2):331 – 363.
12. Rogers JJW, Adams JAS. Uranium and thorium. In Handbook of Geochemistry (ed. Wedepohl K.H.) [C]. Springer Verlag, Berlin 1969; VII-3, 92-B-1 to 92-0-8, 90-B-1 to 90-0-5.
13. Cathelineau M, Holliger P. Polyphase metallogenesis of hydrothermal uranium veins from the southern amoricon massif, France. Proc. Int. Mtg Nancy, 1987; 212-217.
14. Navas A, Sotob J, Machín J. 238U, 226Ra, 210Pb, 232Th and 40K activities in soil profiles of the Flysch sector (Central Spanish Pyrenees). App. Rad. Iso. 2002; 57: 579-589.
15. Hussein AA. Lecture course in nuclear geology, NMA, Egypt 1978; 101.
16. El-Feky MG, El Mowafy AA, Abdel Warith A. Mineralogy, geochemistry, radioactivity and environmental impacts of Gabal Marwa Granites, southeastern Sinai, Egypt. Chin. J. Geochem. 2011; 30: 175-186.
17. Reeves RD, Brooks RR. Trace element analyses of geological materials. John Wiley & sons Inc., New York 1978; 421.
18. Charbonneau BW. Radiometric study of three radioactive granites in the Canadian Shield: Elliot Lake, Ontario; Fort Smith, Fury and Hecla, NWT. In: Maurice YT (ed) Uranium in granites, Geol. Surv. Canada 1982; 91–99.18. Raslan, MF, El-Feky, MG. Radioactivity and mineralogy of the altered granites of the Wadi Ghadir shear zone, South Eastern Desert, Egypt. Chin. J. Geochem. 2012; 31: 30–40.
19. Heinrich EW. Mineralogy and geology of radioactive raw materials, McGraw Hill, New York-Toronto-London 1958; 654.
20. Hogarth DD. Classification and nomenclature of the pyrochlore group. Am. Miner. 1977; 62: 403-410.
21. Khazback AE, Raslan MF. Potentialities of physical up-grading of Gebel Gattar uranium ore, Eastern Desert, Egypt. Al-Azhar Bull. Sci. 1995; 5: 1-7.